Original Article

Diabetes & Vascular Disease Research
July-August 2023: 1–12

DOI: 10.1177/14791641231197106
journals.sagepub.com/home/dvr
Sage

Dapagliflozin attenuates cardiac remodeling and dysfunction in rats with β-adrenergic receptor overactivation through restoring calcium handling and suppressing cardiomyocyte apoptosis

Tao Liu[1,2,3], Jinchun Wu[4], Shaobo Shi[1,2,3], Bo Cui[1,2,3], Feng Xiong[5], Shuang Yang[1,2,3] and Min Yan[1,2,3]

Abstract

Background: Long-term β-adrenergic receptor (β-AR) activation can impair myocardial structure and function. Dapagliflozin (DAPA) has been reported to improve clinical prognosis in heart failure patients, whereas the exact mechanism remains unclear. Here, we investigated the effects of DAPA against β-AR overactivation toxicity and explored the underlying mechanism.

Methods and Results: Rats were randomized to receive saline + placebo, isoproterenol (ISO, 5 mg/kg/day, intraperitoneally) + placebo, or ISO + DAPA (1 mg/kg/day, intragastrically) for 2-week. DAPA treatment improved cardiac function, alleviated myocardial fibrosis, prevented cardiomyocytes (CMs) apoptosis, and decreased the expression of ER stress-mediated apoptosis markers in ISO-treated hearts. In isolated CMs, 2-week ISO stimulation resulted in deteriorated kinetics of cellular contraction and relaxation, increased diastolic intracellular Ca^{2+} level and decay time constant of Ca^{2+} transient (CaT) but decreased CaT amplitude and sarcoplasmic reticulum (SR) Ca^{2+} level. However, DAPA treatment prevented abnormal Ca^{2+} handling and contractile dysfunction in CMs from ISO-treated hearts. Consistently, DAPA treatment upregulated the expression of SR Ca^{2+}-ATPase protein and ryanodine receptor 2 (RyR2) but reduced the expression of phosphorylated-RyR2, Ca^{2+}/calmodulin-dependent protein kinase II (CaMKII), and phosphorylated-CaMKII in ventricles from ISO-treated rats.

Conclusion: DAPA prevented myocardial remodeling and cardiac dysfunction in rats with β-AR overactivation via restoring calcium handling and suppressing ER stress-related CMs apoptosis.

[1]Department of Cardiology, Renmin Hospital of Wuhan University, Wuhan, China
[2]Cardiovascular Research Institute, Wuhan University, Wuhan, China
[3]Hubei Key Laboratory of Cardiology, Wuhan, China
[4]Department of Cardiology, Qinghai Provincial People's Hospital, Xining, China
[5]Montreal Heart Institute (MHI), Department of Medicine, Faculty of Medicine, Université de Montréal, Montreal, QC, Canada

Corresponding authors:
Tao Liu, Department of Cardiology, Renmin Hospital of Wuhan University, zhangzhidong road 99, Wuhan, 430060, China.
Email: taoliu@whu.edu.cn

Jingchun Wu, Department of Cardiology, Qinghai Provincial People's Hospital, No.2 Gong He Road, Xining 810007, China.
Email: wujinchun117@sina.com

Shaobo Shi, Department of Cardiology, Renmin Hospital of Wuhan University, Zhangzhidong Road 99, Wuhan 430060, China.
Email: shiyige@whu.edu.cn

Keywords
Dapagliflozin, β-adrenergic receptor, cardiac function, myocardial fibrosis, apoptosis, calcium handling

Introduction

Heart failure (HF) is associated with high morbidity and mortality.[1] Sustained activation of sympatho-β-adrenergic system, a powerful regulator of heart physiological functions, has been observed in HF patients.[2,3] The long-term effect of β-adrenergic receptor (β-AR) activation on cardiovascular function is harmful, including distinct myocardial remodeling and severe cardiac dysfunction.[4,5] It is well-accepted that chronic stimulation with isoproterenol (ISO), a non-selective agonist of β-AR, can mimic sustained β-AR activation in experimental studies.[6,7] Emerging evidence suggests that severe cardiomyocyte (CM) apoptosis and abnormal Ca^{2+} handling are implicated in the etiopathogenesis of chronic ISO stimulation-induced cardiomyopathy.[8–10]

Dapagliflozin (DAPA), a selective inhibitor of sodium/glucose cotransporter-2 inhibitor (SGLT2i), is a novel anti-hyperglycaemic drug that blocks the glucose reabsorption in renal proximal tubules.[11] Improved cardiac function in HF patients with DAPA appears to be independent of the effect on glycaemia, whereas the exact mechanisms are still poorly understood.[12] Our previous studies confirmed that DAPA treatment improved right ventricular function and prevented ventricular arrhythmia by restoring Ca^{2+} handling in rats with right HF.[13] In addition, the anti-apoptosis effect of DAPA has been observed in various animal models.[14–16] Therefore, we hypothesize that given its effects on normalizing $[Ca^{2+}]_i$ homeostasis and preventing cell apoptosis, DAPA might exert a cardioprotective effect against chronic β-AR activation-induced myocardial damage and cardiac dysfunction. In the present study, we tested this hypothesis using a rat model of chronic ISO administration.

Materials and methods

Experimental animals

Animal care and use were performed in accordance with the guidelines of the American Veterinary Medical Association (AVMA) for the Euthanasia of Animals (2020). All the experimental procedures were approved by the Animal Research Ethics Committee of Renmin Hospital of Wuhan University (No.20201211). Adult Sprague-Dawley rats (8 weeks, male, weighting from 240 to 300 g) were purchased from the Animal Centre of Wuhan University. After 1 week, animals were randomly divided into one of three groups: the control (CTL) group where rats were treated with intraperitoneal (i.p.) injection of saline (0.1 mL/kg/d) plus intragastric (i.g.) administration of placebo; the ISO group where rats were treated with ISO (Sigma, USA) (5 mg/kg/d, i. p.) plus placebo (i.g.); the ISO + DAPA group where rats were treated with ISO (5 mg/kg/d, i. p.) plus DAPA (1 mg/kg/d, i. g.). The duration of drug administration was two consecutive weeks.

Echocardiographic analysis

At the end of 14-day drug treatment period, cardiac function was blindly assessed using a transthoracic echocardiography system (VINNO Technology, Suzhou, China). M-mode tracing was performed to measure the left ventricular (LV) posterior wall dimension in diastole (LVPWD), LV end-systolic diameter (LVESD), interventricular septum thickness at diastole (IVSD), LV ejection fraction (LVEF), LV end-diastolic diameter (LVEDD), LV fractional shortening (LVFS), and cardiac output (CO).

Analysis of N-terminal pro-brain natriuretic peptide (NT-pro-BNP)

As previously described,[13] serum NT-pro-BNP levels were determined using an ELISA kit (ELK Biotechnology. Ltd, Wuhan).

Histological analysis

As previously described,[13] LV myocardial fibrosis was evaluated using Masson's trichrome staining. The interstitial collagen volume fraction (CVF) was calculated as collagen area/reference area ×100%.

Detection of the apoptosis of LV cardiomyocytes (LVCMs) by the TUNEL staining

As previously described.[17] TUNEL staining was used to assess LV myocardial apoptosis, and the apoptosis rate was calculated as the percentage of positive apoptotic CMs nuclei/total CMs nuclei.

LVCMs Isolation

As previously described,[18] LVCMs were obtained from rat hearts through enzymatic digestion with collagenase type II. Briefly, rats were anesthetized (pentobarbital sodium, 40 mg/kg, i. p.) and heparinized (heparin sodium, 1000 U, i. p.). Subsequently, heart was quickly isolated and cannulated by the aorta in a Langendorff system. The heart was

perfused sequentially with the following buffers: (1) normal Tyrode solution at 37°C for 10-15 min to recover regular spontaneous rhythm, (2) Ca^{2+}-free Tyrode solution for 15–20 min, and (3) Ca^{2+}-free Tyrode solution containing collagenase type II (0.8 mg/ml, Worthington) plus 0.1% bovine serum albumin for 6–8 min at 37°C for another 10 min. After digestion, LV tissue was cut into fragments and gently agitated in Ca^{2+}-free Tyrode solution plus 1 mg/ml bovine serum albumin to dissociate and collect LVCMs. Finally, ventricular cells were filtered using a nylon mesh (pore size 200mm) and subjected to a progressive normalization of Ca^{2+} levels to a final concentration of 1.8 mM. Normal Tyrode solution contained (in mM): NaCl 130, KCl 5.4, $CaCl_2$ 1.8, $MgCl_2$ 1.0, NaH_2PO4 0.33, glucose 10 and HEPES 10 (pH was adjusted to 7.4 with NaOH). The free Ca^{2+}-Tyrode's solution was the normal Tyrode's solution without CaCl2. LVCMs were kept in normal Tyrode solution at room temperature and used within 6 h following isolation.

Measurement of cell contraction

LVCMs were superfused with normal Tyrode solution. Cell contraction was recorded in LVCM using a video camera (IonOptix Corporation, Milton, MA, USA) at 240 Hz as previously described.[19] Fractional cell-shortening (%), time to half relaxation of shortening (THRS), and time to peak shortening (TPS) were calculated to assess cell contractility.

Ca^{2+} imaging study in LVCMs

To record Ca^{2+} transient (CaT), LVCMs were incubated with fluorescent indicator (Fura-2 a.m., 5 μM) at room temperature for 20–25 min. Subsequently, cells were superfused with normal Tyrode solution for another 30 min to remove extracellular Fura-2 a.m. and ensure complete deesterification of intracellular Fura-2 a.m. In this study, Fura-2 was excited by 340 nm and 380 nm μStep light source, and emission was recorded at 510 nm. In order to provide an index of intracellular Ca^{2+} ($[Ca^{2+}]_i$) level, the ratio of 340/380-nm fluorescence was calculated following background fluorescence subtraction. CaTs were recorded in LVCMs with 1 Hz electrically field stimulation at 37°C. As previously described,[13,20] the amplitude of CaT, the diastolic $[Ca^{2+}]_i$ level, as well as CaT decay time constant were measured to evaluate cellular Ca^{2+} handling. Additionally, the sarcoplasmic reticulum (SR) Ca^{2+} content ($[Ca^{2+}]_{SR}$) was measured by rapidly adding caffeine (10 mm) after a train of 1 Hz electrically field stimulation. The caffeine-induced CaT amplitude was calculated to evaluate $[Ca^{2+}]_{SR}$. All measurements were acquired and analyzed with IonWizard 6.2 software (IonOptix Corporation, Milton, MA, USA).

Western blot analysis

Proteins were extracts from LV tissues and then the concentration of protein was detected by BCA protein assay kit. An equal amount of protein was separated by using a 10% SDS-PAGE and transferred to PVDF membranes. The membrane was blocked with non-fat dried milk for 30 min at 37°C and then incubated with the primary antibodies [anti-glucose-regulated protein 78 (GRP78; 1:3000; Servicebio, GB11098,Wuhan, China), anti-phosphorylated protein kinase R-like ER kinase (p-PERK; 1:3000; Servicebio, GB11510, China), anti-activating transcription factor-4 (ATF-4;1:2000; Affinity, DF6008, USA), anti-phosphorylated eukaryotic translation initiation factor 2α (p-eIF2α; 1:3000; BIOSS, BS-4842R, USA), anti-C/EBP homologous protein (CHOP; 1:2000; Proteintech, 60304-1-IG; China), anti-cleaved caspase-12 (C-Casp-12; 1:3000; Abcam, AB62484, UK), total ryanodine receptor 2 (t-RyR; 1:1000; Affinity, AF0015, USA), Ser2814-phosphorylated RyR2 (Ser2814-p- RyR2;1:1000; Affinity, AF0015, USA), SR Ca^{2+}-ATPase 2a (SERCA2a; 1:3000; Servicebio, GB112211, China), phospholamban (PLB; 1:1000; BIOSS, BS-4197R, USA), total CaMKII (t-CaMKII; 1:3000; Abcam, AB52476, USA), and Thr287-phosphorylated CaMKII (p-CaMKII; 1:1000; Cell Signaling Technology, 12716, USA)] overnight at 4°C. After being washed with Tris-buffered saline and Tween for three times, membranes were incubated with corresponding secondary antibodies conjugated to horse radish peroxidase for 1 h at 37°C. The protein bands were visualized by chemiluminescence detection using an ECL kit and films were scanned and analyzed with Quantitive One version four software (Bio-Rad, Hercules, CA, USA). The protein contents were normalized to that of glyceraldehyde-3-phosphate dehydrogenase (GAPDH).

Statistical analysis

In this study, all study data were analysed using IBM SPSS 17.0 or GraphPad Prism 5.0. The data were presented as the mean ± SEM and then analyzed by ANOVA followed by Tukey's post hoc test to determine the differences among three groups. A value of $p < .05$ was considered statistically significant.

Results

DAPA Attenuated Cardiac Structural Remodeling and Dysfunction in Rat Hearts with Chronic ISO Stimulation

Table 1 shows the echocardiographic parameters and NT-proBNP levels of three groups. Increased LVPWD, LVEDD, LVESD, and IVSD but decreased LVEF, LVFS, and CO were observed in ISO group when compared with CTL group (all

Table 1. Results of echocardiographic parameters and NT-pro-BNP.

	CTL	ISO	ISO+DAPA
LVPWD (mm)	2.05 ± 0.09	2.64 ± 0.21*	2.13 ± 0.13#
LVEDD (mm)	5.94 ± 0.13	8.28 ± 0.08*	6.54 ± 0.06#
LVESD (mm)	3.53 ± 0.13	5.83 ± 0.13*	4.28 ± 0.14#
IVSD (mm)	1.96 ± 0.11	2.53± 0.08*	2.17 ± 0.13#
LVEF (%)	76.28 ± 3.28	43.82 ± 4.34*	56.48 ± 3.35#
LVFS (%)	42.12 ± 2.63	28.23 ± 3.57*	33.52 ± 4.56#
CO (ml/min)	351.14 ± 32.36	303.58 ± 47.61*	336.28 ± 23.52#
NT-pro-BNP (ng/ml)	1.22 ± 0.27	3.24 ± 0.48*	2.36 ± 0.24#

LVPWD: left ventricular posterior wall dimensions in diastole; LVEDD: left ventricular end-diastolic diameter; LVESD: left ventricular end-systolic diameter, LVEF: left ventricular ejection fraction, LVFS: left ventricular fractional shortening, IVSD: interventricular septum thickness at diastole; CO: cardiac output; NT-pro-BNP: N-terminal pro-Brain natriuretic peptide.
Data are presented as the mean± SEM. *p* values were calculated using a one-way analysis of variance test and Tukey's multiple comparisons test used for multiple comparisons. *N* = 5 per group.
*$p<.05$, indicates statistical significance compared with the CTL group.
#$p<.05$, indicates statistical significance compared with the ISO group.

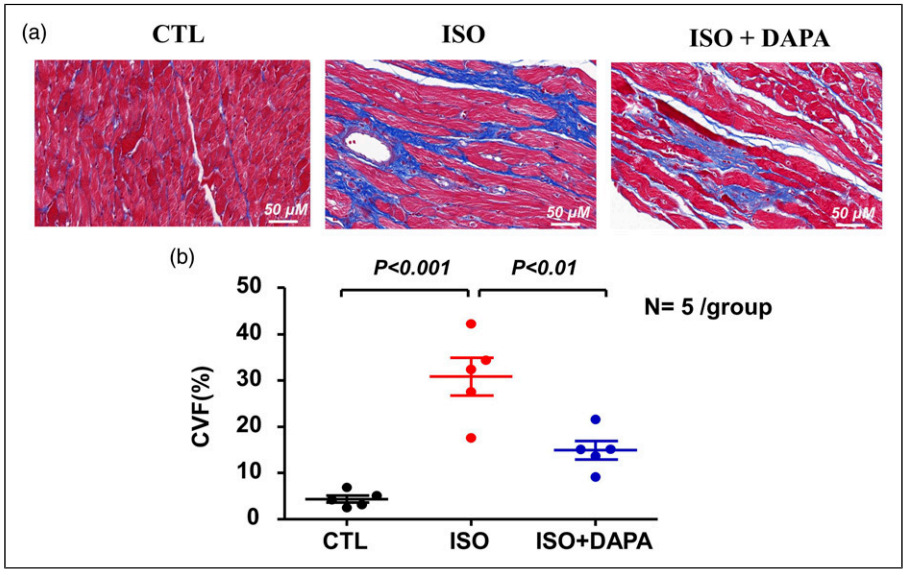

Figure 1. DAPA reduced left ventricular (LV) myocardial fibrosis: (a) Representative images of the LV histological tissues stained with Masson's trichrome from one rat in each group (magnification of ×400); (b) Quantitative analysis of LV myocardial fibrosis in each group. Horizontal lines show the mean± SEM. *N* = 5 per group for all analyses. CVF: collagen volume fraction; DAPA: dapagliflozin; ISO: isoproterenol.

$p < .01$). Additionally, 2-week ISO stimulation significantly increased NT-pro-BNP level in rats from ISO group ($p <$ .01 vs CTL group). However, DAPA treatment attenuated the abnormal echocardiographic indices and NT-pro-BNP level induced by 2-week ISO exposure (all $p < .05$).

DAPA Prevented myocardial fibrosis and apoptosis induced by chronic ISO stimulation in rat hearts

Figure 1 shows the representative results of Masson staining in three groups. Consistent with echocardiographic results, LV interstitial CVF was also markedly augmented in the ISO group when compared to that in the CTL group (ISO group: 30.80 ± 4.07% vs CTL group: 4.37 ± 0.77%, $p < .001$). In contrast, a lower LV interstitial CVF was found in ISO+DAPA group (ISO+DAPA: 14.94 ± 1.99% vs ISO group: 30.80 ± 4.07%, $p < .01$).

Figure 2 shows the representative results of TUNEL staining in left ventricles from each group. The myocardial apoptotic rate was significantly augmented in the ISO group when compared to that in the CTL group (ISO group: 54.3 ± 4.6% vs CTL group: 0.6 ± 0.1%, $p < .01$). However, compared with ISO group, chronic DAPA administration

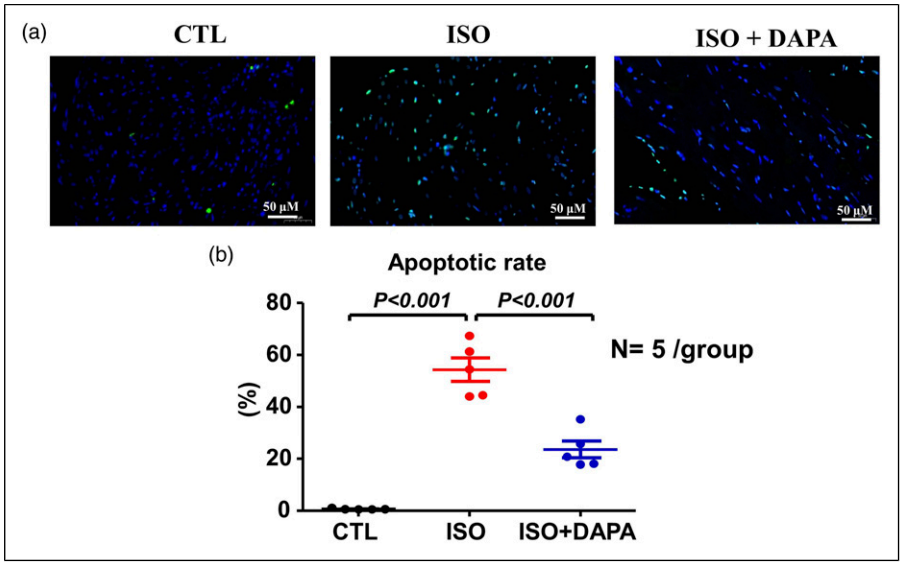

Figure 2. DAPA reduced myocardial apoptosis: (a) TUNEL stain shown (magnification of ×400) in the LV tissues from three groups; (b) Summarized data of myocardial apoptosis rate in each group. Horizontal lines show the mean± SEM. *N* = 5 per group for all analyses.

markedly reduced the myocardial apoptotic rate by 57% in ISO+DAPA group (ISO+DAPA: 23.5 ± 3.2% vs ISO group: 54.3 ± 4.6%, $p < .01$).

DAPA restored LVCMs contractility and relaxant function in ISO-treated rats

Figure 3 summarizes the mechanical properties of isolated LVCMs from each group. 2-week ISO stimulation significantly decreased fraction cell-shortening by 63% in ISO group when compared with CTL group (ISO group: 4.40 ± 0.40% vs CTL group: 11.97 ± 0.49%, $p < .001$). Additionally, the TPS (ISO group: 346.6 ± 20.4 ms vs CTL group: 140.3 ± 14.1 ms) and THRS (ISO group: 121.2 ± 8.5 ms vs CTL group: 57.1 ± 3.7 ms) were prolonged by 147% and 112% in ISO group, respectively (all $p < .001$ vs CTL). However, DAPA treatment improved the cardiomyocyte contractile and relaxant function in ISO+DAPA group, evident by increased fraction cell-shortening but decreased TPS and THRS (all $p < .001$ vs ISO group).

DAPA improved CaT and preserved [Ca2+]SR in LVCMs from rats with 2-week ISO stimulation

Typical recordings of CaTs are shown in Figure 4(a). Compared with CTL group, the decay time constant of CaT (454.30 ± 22.80 ms in ISO group vs. 154.90 ± 17.19 ms in CTL group) and diastolic $[Ca^{2+}]_i$ level (1.22 ± 0.04 in ISO group vs. 0.83 ± 0.03 in CTL group) were significantly increased while the CaT amplitude was markedly reduced (0.19 ± 0.02 in ISO group vs. 0.38 ± 0.01 in CTL group) in ISO group (all $p<.01$). However, abnormal changes in CaT induced by chronic ISO exposure were prevented by DAPA treatment in ISO +DAPA group (all $p < .01$ vs ISO group; Figure 4(b)).

In our study, the change in $[Ca^{2+}]_{SR}$ was determined by recording caffeine-induced CaT (Figure 5(a)). We found that 2-week ISO stimulation markedly decreased $[Ca^{2+}]_{SR}$ by 48% in LVCMs isolated from ISO group (ISO group: 0.54 ± 0.04 vs. CTL group: 1.04 ± 0.05, $p < .001$; Figure 5(b)). In contrast, DAPA treatment increased $[Ca^{2+}]_{SR}$ by 57% in ISO +DAPA group (ISO+DAPA group: 0.85 ± 0.04 vs. ISO group: 0.54 ± 0.04, $p < .001$; Figure 5(b)).

DAPA ameliorated abnormal expression of major Ca2+ handling proteins

As shown in Figure 6, the protein levels of p-CaMKII, t-CaMKII, and p-RyR2 were markedly upregulated in LV tissues from ISO group (all $p < .01$ vs CTL group). However, the protein expression of t-RyR2 and SERCA2a were significantly lower in ISO group than those in CTL group (all $p < .01$). Additionally, DAPA treatment significantly preserved the expression of RyR2 and SERCA2a but reduced the expression of p-CaMKII, p-RyR2, and t-CaMKII in the ISO + DAPA group (all $p < .01$ vs ISO group). There was no significant difference in terms of PLB expression among three groups ($p > .05$).

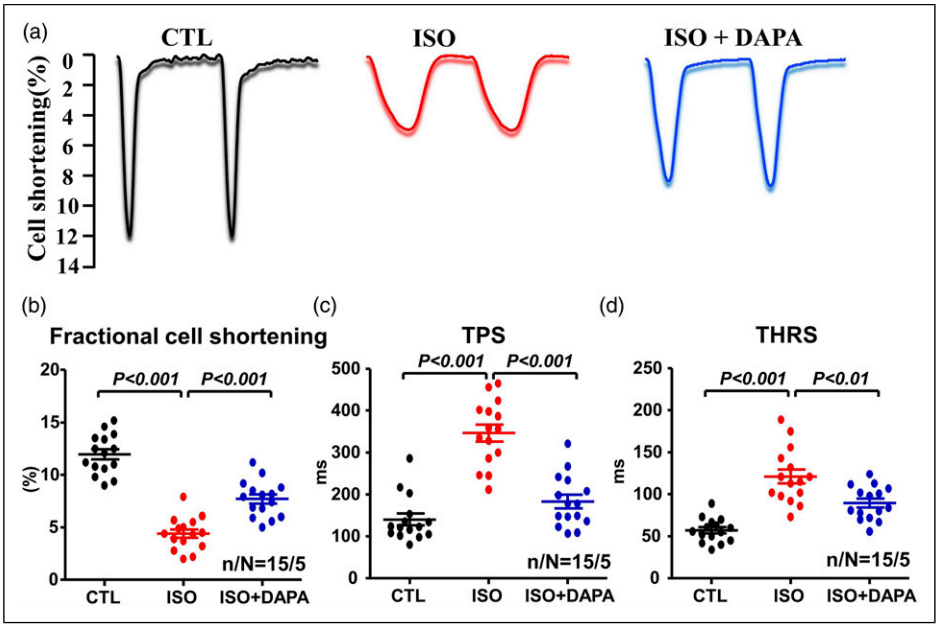

Figure 3. Effect of DAPA on ventricular calcium transient (CaT): (a) The typical recording of CaT in each group; (b) Diastolic intracellular Ca^{2+} level; (c) CaT amplitude; (d) CaT decay time constant. Horizontal lines show the mean± SEM. *n/N* = 15/5 (15 LVCMs from five rat hearts per group) for all analyses.

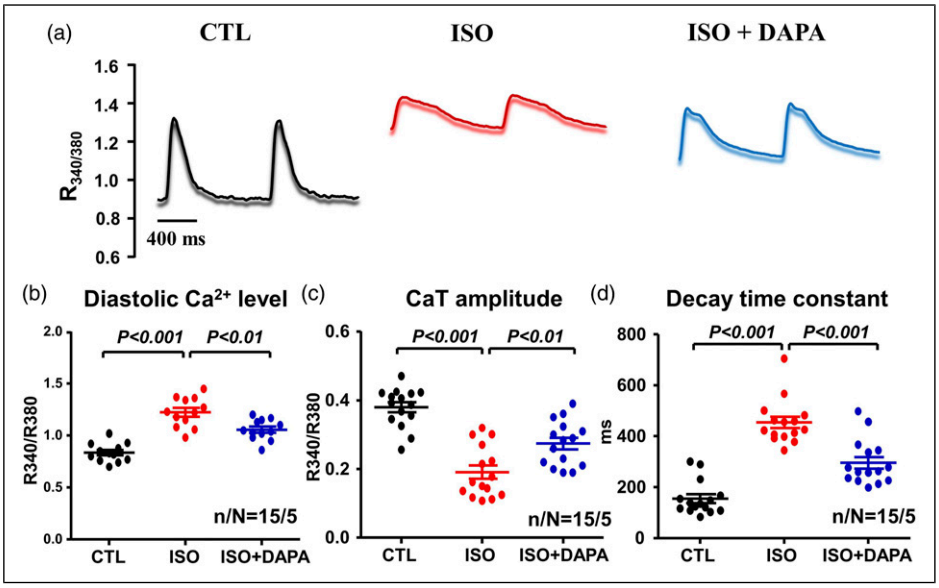

Figure 4. Effect of DAPA on ventricular cardiomyocytes contractility: (a) The typical recordings of cell shortening in each group; (b) Quantitative analysis of fractional cell shortening, (c) TPS (time to peak shortening), and (d)THRS (time to half relaxation of shortening) in LVCMs from three groups. Horizontal lines show the mean± SEM. *n/N* = 15/5 (15 LVCMs from five rat hearts per group) for all analyses.

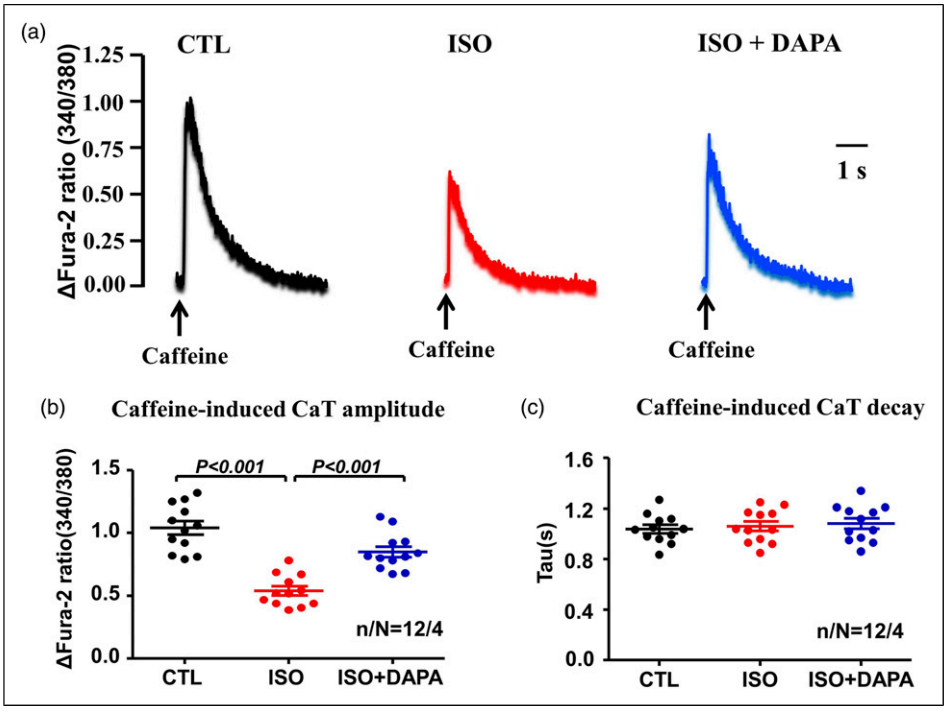

Figure 5. Effect of DAPA on sarcoplasmic reticulum (SR) Ca^{2+} content: (a): The typical recording of caffeine induced-calcium transient in each group; (b) The comparison of caffeine-induced CaT amplitude and (c) decay time constant in LVCMs from three groups. Horizontal lines show the mean± SEM. *n*/*N* = 12/4 (12 LVCMs from four rat hearts per group) for all analyses.

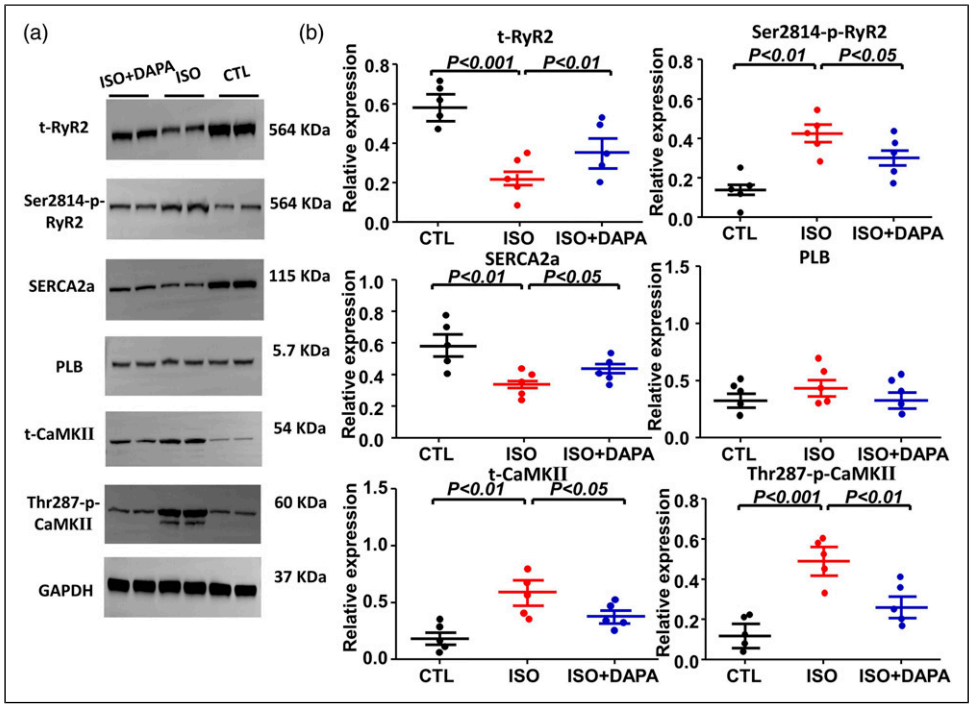

Figure 6. Effect of DAPA on expression of key calcium handling proteins: (a) Representative results of western blots from two ventricles in each group; (b) Quantitative analysis of key calcium handling proteins expression in each group. Horizontal lines show the mean± SEM. *N* = 5 per group for all analyses.

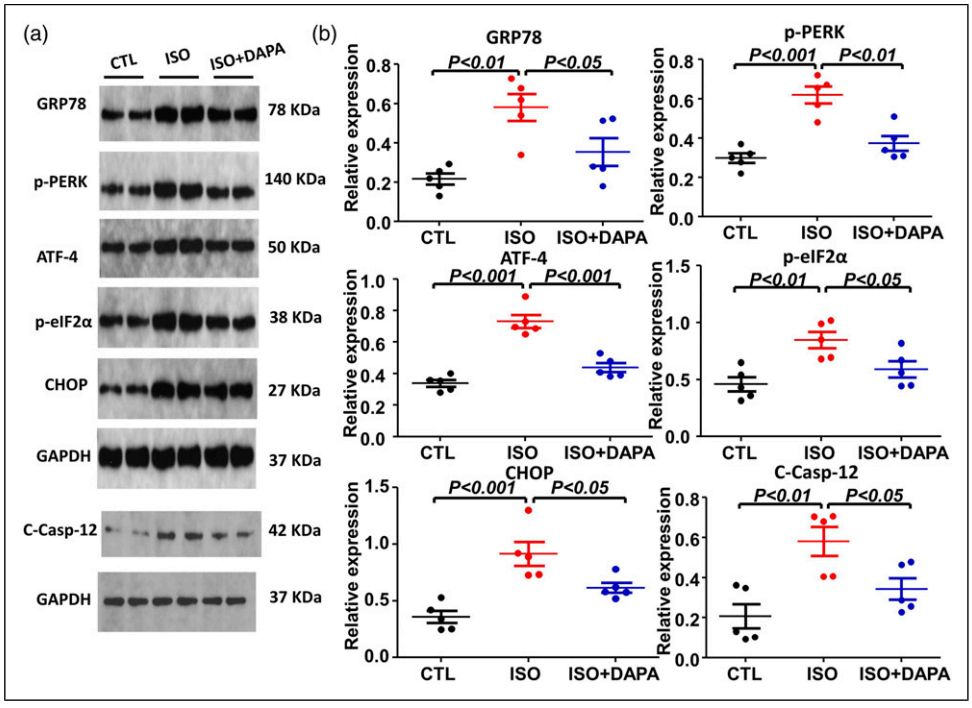

Figure 7. Effect of DAPA on expression of ER stress-mediated apoptosis markers. (a) Examples of original gels from two ventricles in each group. (b) LV expression of ER stress-mediated apoptosis markers in each group. Horizontal lines show the mean± SEM. *N* = 5 per group for all analyses.

DAPA Inhibited Endoplasmic Reticulum (ER) Stress-mediated Apoptotic Signal in Rat Hearts with Chronic ISO Stimulation

To further determine the effects of DAPA on the apoptotic signal, we detected the protein expression of an ER stress biomarker (GRP78) and compensatory unfolded protein response (UPS) pathway (PERK/eIF2α/ATF-4) and ER stress-related pro-apoptosis factors (CHOP and C-Casp-12) in each group. 2-week ISO stimulation markedly up-regulated the protein expression of p-PERK, p-eIF2α, CHOP, ATF-4, GRP78, and C-Casp-12 in ISO group (all $p < .01$ vs CTL group; Figure 7). However, DAPA treatment markedly decreased the protein expression of p-PERK, p-eIF2α, CHOP, ATF-4, GRP78, and C-Casp-12 in the ISO+DAPA group (all $p < .05$ vs ISO group; Figure 7).

Discussion

In this study, we investigated the effects of DAPA treatment on chronic β-AR activation-mediated myocardial remodeling and cardiac dysfunction in rats and the underlying mechanisms for actions. Our results show that (1) treatment with DAPA attenuated LV structural remodeling and dysfunction in rats with β-AR overactivation; (2) DAPA treatment prevented LV fibrosis and LVCMs apoptosis in rats with 2-week ISO stimulation; (3) DAPA treatment restored Ca^{2+} handling in LVCMs from sustained ISO-treated hearts by increasing CaT amplitude, reducing diastolic $[Ca^{2+}]_i$ level, shortening decay time constant of CaT, and preserving $[Ca^{2+}]_{SR}$; (4) DAPA treatment caused significant increases in the protein levels of t-RyR2 and SERCA2a but a reduction of protein expression of p-RyR2, CaMKII, and p-CaMKII in LV samples from ISO-treated rats; (5) DAPA treatment suppressed ER stress-mediated apoptosis induced by 2-week ISO exposure in rat hearts, evident by downregulated expression of p-PERK, GRP78, ATF-4, CHOP, C-Casp-12, and p-eIF2α protein expression.

ER Stress-mediated apoptosis and β-AR overactivation in cardiomyocytes

We observed that sustained β-AR stimulation increased the protein expression of p-eIF2a, GRP78, ATF-4, CHOP, p-PERK, and C-Casp-12 in LV tissues of rat hearts, indicating that aberrant ER stress-related apoptosis occurred during the process of β-AR overactivation. Previous studies also confirmed that sustained β-AR stimulation could promote ER stress-mediated apoptosis in cardiac myocytes. Ni et al.[21] Reported that 2 weeks of ISO administration (5 mg/kg/d) resulted in sustained ER stress and myocardial apoptosis in rat hearts. Moreover, in isolated

adult rat ventricular CMs, sustained β-AR activation by ISO for 1 day significantly upregulated the protein levels of ER stress markers and cell apoptosis.[22] Thus, our results confirm previous studies and suggest that β-AR overactivation-induced ER stress and associated apoptosis is reliable and reproducible.

DAPA restored proper Ca^{2+} handling in LVCMs from rats with sustained β-AR stimulation

Many studies showed that β-AR stimulation by ISO could induce aberrant intracellular Ca^{2+} homeostasis in CMs.[5,23,24] In the current study, we also found that chronic ISO stimulation impaired Ca^{2+} handling in LVCMs from rats, as demonstrated by enhanced diastolic $[Ca^{2+}]_i$ level, prolonged decay time constant of CaT, reduced CaT amplitude and $[Ca^{2+}]_{SR}$, whereas DAPA treatment abrogated there abnormal alterations of Ca^{2+} handling. Moreover, our present study also demonstrated that β-AR overactivation could reduce the expression of SERCA2a in rat hearts, whereas DAPA treatment preserved it. It is well-known that SERCA2a pump is an important protein responsible for cytosolic Ca^{2+} reuptake into SR during diastole in CMs.[25] It is suggested that SERCA2a pump dysfunction, resulting from reduced SERCA2a expression or activity, could result in an enhanced diastolic $[Ca^{2+}]_i$ concentration and a depleted $[Ca^{2+}]_{SR}$.[23,25,26] In addition, a depleted $[Ca^{2+}]_{SR}$ can finally lead to a reduction of Ca^{2+} release during systolic period.[25,26] Thus, we speculate that DAPA restored proper intracellular Ca^{2+} homeostasis in the present study partly due to the preservation of SERCA2a expression.

Furthermore, it is proposed that increased diastolic SR Ca^{2+} leak due to abnormal activation of RyR2 is associated with β-AR stimulation-induced aberrant Ca^{2+} homeostasis in CMs.[27,28] Previous studies suggested that upregulated CaMKII-dependent RyR2 phosphorylation is implicated in abnormal opening of RyR2 channel during diastole and hence to increase diastolic SR Ca^{2+} leak.[29–31] In isolated murine and human failing CMs, DAPA has been shown to decreased diastolic SR Ca^{2+} leak via preventing CaMKII-dependent RyR2 phosphorylation.[31,32] Similarly, in a rat model of pulmonary arterial hypertension, we demonstrated that 5-week DAPA treatment reduced diastolic SR Ca^{2+} leak in right ventricular CMs via preventing the activation of CaMKII/p-RyR2 pathway.[13] In this study, DAPA treatment downregulated the protein levels of CaMKII, p-CaMKII and p-RyR2 in chronic ISO-treated hearts, indicating an inhibition of CaMKII/p-RyR2 pathway by DAPA treatment. Thus, it is suggested that the suppression of CaMKII/p-RyR2 pathway might be associated with DAPA improved Ca^{2+} handling in the present study.

DAPA alleviate ER stress-related apoptosis induced by β-AR overactivation via restoring $[Ca^{2+}]i$ homeostasis

Our present results showed that DAPA treatment decreased the protein expression of ER stress-mediated apoptosis markers as well as attenuated LVCMs apoptosis in rat hearts with β-AR stimulation, suggesting that ER stress and the associated apoptosis are diminished by DAPA in vivo.

Ample studies suggest a role for abnormal $[Ca^{2+}]_i$ homeostasis in the trigger of the ER stress-mediated apoptotic pathway. Dong et al.[33] reported that $[Ca^{2+}]_i$ overload and depletion of $[Ca^{2+}]_{SR}$ could result in prolonged ER stress and associated apoptosis in neonatal CMs that had undergone ischemia/reperfusion injury. Moreover, George et al.[34] found that ER stress could be induced by abnormal Ca^{2+} homeostasis in a canine model of chronic heart failure (CHF). Similarly, Castillero et al.[35] demonstrated that A23187 (a calcium ionophore) and thapsigargin (an inhibitor of SERCA2a) decreased $[Ca^{2+}]_{SR}$ and thereby promoted the ER stress-mediated apoptosis in a human adult LVCMs-like cell line. In contrast, the restoration of normal $[Ca^{2+}]_i$ homeostasis by certain drugs or interventions is beneficial for the prevention of ER stress and the associated apoptosis in human and animal hearts.[34–36] In this study, DAPA treatment abrogated abnormal $[Ca^{2+}]_i$ homeostasis caused by chronic ISO stimulation, which may be the important action of DAPA to attenuate β-AR overactivation-induced ER stress and associated apoptosis.

DAPA attenuated β-AR overactivation-induced cardiac dysfunction via suppressing ER stress-mediated apoptosis and promoting calcium handling

As shown in previous studies,[5,37–40] we also observed that chronic β-AR activation by ISO induced cardiac dysfunction and myocardial structural remodeling in rat hearts, which were all attenuated by DAPA treatment. Apoptosis has been suggested to contribute to the loss of terminally differentiated CMs and thereby promote the progression of cardiac structural and function remodeling in cardiovascular diseases.[41] Since the regenerative capacity of the myocardium is limited, apoptosis is a promising therapeutic target for the improvement of cardiac function. ER stress-mediated apoptosis is a main apoptotic signaling pathway in the cardiovascular system.[41] It is proposed that the suppression of ER stress-associated apoptosis could prevent ISO-induced cardiac dysfunction in animal hearts.[38,42] In this study, DAPA suppressed ISO-induced ER stress and the associated apoptosis, which may be the important action of DAPA to

provide a protective effect against ISO-induced cardiac dysfunction.

Furthermore, intracellular Ca^{2+} mishandling can directly lead to abnormal cardiac function.[43] In the present study, DAPA treatment improved CaT, decreased $[Ca^{2+}]_i$ overload, and preserved $[Ca^{2+}]_{SR}$ in CMs from rats that had undergone chronic ISO stimulation. A similar result was obtained in a previous study, which demonstrated that the 5-week administration of DAPA normalized calcium handling to improve cardiac function in a right heart failure rat model.[13] Thus, it is suggested that DAPA attenuated β-AR overactivation-induced cardiac dysfunction via directly promoting calcium handling.

Clinical implication

Chronic hyperactivation of β-AR due to increased sympathetic nervous system activity has been involved in the pathophysiological progression of CHF.[44] Although β-AR blockers are the mainstay of CHF management in clinical practice, side effects of β-AR blockers adversely affect the quality of life and thereby limit their use in certain patients.[45] It is necessary to seek more appropriate drugs for CHF patients who are intolerable to β-AR blockers. In the present study, we observed that DAPA administration attenuated ER stress-related apoptosis and restored proper Ca^{2+} handling in rat hearts with chronic ISO stimulation, indicating that DAPA might be a potential drug for preventing β-AR overactivation-induced cardiac dysfunction.

Study limitations

There are several limitations in our study. First, we did not assess the effect of DAPA treatment on SR Ca^{2+} leak via recording diastolic Ca^{2+} spark or determining tetracaine-induced reduction of $[Ca^{2+}]_i$. Second, based on previous studies,[46–48] we determined the dose of DAPA (1 mg/kg/day) intervention in the present study, which is higher than clinical dose. We only assessed the effects of DAPA (1 mg/kg/day) treatment over a 2-week time course, whereas its effects at various doses and/or other time points need to be investigated in future studies. Finally, the effect of DAPA treatment on CMs in vitro has not been investigated in this study.

Conclusions

Our study demonstrates that DAPA treatment prevented myocardial remodeling and cardiac dysfunction in rats with β-AR overactivation, which may be related to restored calcium handling and suppressed ER stress-related cardiomyocyte apoptosis.

Author contributions

T L and JW contributed to conception and design, analysis, drafted the article, gave final approval, and agreed to be accountable for all aspects of work ensuring integrity and accuracy. SS contributed to conception, acquisition and interpretation, drafted the article, gave final approval, and agreed to be accountable for all aspects of work ensuring integrity and accuracy. BC and FX contributed to design, acquisition and interpretation, critically revised the article, gave final approval, and agreed to be accountable for all aspects of work ensuring integrity and accuracy. SY and MY contributed to acquisition, analysis, and interpretation, gave final approval, and agreed to be accountable for all aspects of work ensuring integrity and accuracy.

Declaration of conflicting interests

The author(s) declared no potential conflicts of interest with respect to the research, authorship, and/or publication of this article.

Funding

The author(s) disclosed receipt of the following financial support for the research, authorship, and/or publication of this article: This work was supported by the National Natural Science Foundation of China (Grant No. 82270365) and the Application and Basic Research Project from the Science and Technology Department of Qinghai Province (Grant No. 2022-ZJ-758).

Institutional review board statement

The animal study protocol was approved by the Animal Ethics Committee of Renmin Hospital of Wuhan University, China (NO.20201211).

ORCID iD

Tao Liu https://orcid.org/0009-0006-6626-9813

References

1. Writing Committee M and Members AAJC. 2022 AHA/ACC/HFSA Guideline for the Management of Heart Failure. *J Card Fail*. 2022, 28, e1-e167.
2. Esler M, Kaye D, Lambert G, et al. Adrenergic nervous system in heart failure. *Am J Cardiol* 1997; 80: 7L–14L.
3. Bencivenga L, Liccardo D, Napolitano C, et al. beta-Adrenergic Receptor Signaling and Heart Failure: From Bench to Bedside. *Heart Fail Clin* 2019; 15: 409–419.
4. Soltysinska E, Olesen SP and Osadchii OE. Myocardial structural, contractile and electrophysiological changes in the guinea-pig heart failure model induced by chronic sympathetic activation. *Exp Physiol* 2011; 96: 647–663.
5. Liu T, Shi SB, Qin M, et al. Effects of Dantrolene Treatment on Ventricular Electrophysiology and Arrhythmogenesis in Rats With Chronic beta-Adrenergic Receptor Activation. *J Cardiovasc Pharmacol Therapeut* 2015; 20: 414–427.

6. Allawadhi P, Khurana A, Sayed N, et al. Isoproterenol-induced cardiac ischemia and fibrosis: Plant-based approaches for intervention. *Phytother Res* 2018; 32: 1908–1932.
7. Nichtova Z, Novotova M, Kralova E, et al. Morphological and functional characteristics of models of experimental myocardial injury induced by isoproterenol. *Gen Physiol Biophys* 2012; 31: 141–151.
8. Zhao F, Fu L, Yang W, et al. Cardioprotective effects of baicalein on heart failure via modulation of Ca(2+) handling proteins in vivo and in vitro. *Life Sci* 2016; 145: 213–223.
9. Nakayama H, Chen X, Baines CP, et al. Ca2+- and mitochondrial-dependent cardiomyocyte necrosis as a primary mediator of heart failure. *The Journal of clinical investigation* 2007; 117: 2431–2444.
10. Karam S, Margaria JP, Bourcier A, et al. Cardiac Overexpression of PDE4B Blunts beta-Adrenergic Response and Maladaptive Remodeling in Heart Failure. *Circulation* 2020; 142: 161–174.
11. Kasichayanula S, Liu X, Lacreta F, et al. Clinical pharmacokinetics and pharmacodynamics of dapagliflozin, a selective inhibitor of sodium-glucose co-transporter type 2. *Clin Pharmacokinet* 2014; 53: 17–27.
12. Petrie MC, Verma S, Docherty KF, et al. Effect of Dapagliflozin on Worsening Heart Failure and Cardiovascular Death in Patients With Heart Failure With and Without Diabetes. *JAMA* 2020; 323: 1353–1368.
13. Wu J, Liu T, Shi S, et al. Dapagliflozin reduces the vulnerability of rats with pulmonary arterial hypertension-induced right heart failure to ventricular arrhythmia by restoring calcium handling. *Cardiovasc Diabetol* 2022; 21: 197.
14. Elkazzaz SK, Khodeer DM, El Fayoumi HM, et al. Role of sodium glucose cotransporter type 2 inhibitors dapagliflozin on diabetic nephropathy in rats; Inflammation, angiogenesis and apoptosis. *Life Sci* 2021; 280: 119018.
15. El-Shafey M, El-Agawy MSE, Eldosoky M, et al. Role of Dapagliflozin and Liraglutide on Diabetes-Induced Cardiomyopathy in Rats: Implication of Oxidative Stress, Inflammation, and Apoptosis. *Front Endocrinol* 2022; 13: 862394.
16. Hu Y, Xu Q, Li H, et al. Dapagliflozin Reduces Apoptosis of Diabetic Retina and Human Retinal Microvascular Endothelial Cells Through ERK1/2/cPLA2/AA/ROS Pathway Independent of Hypoglycemic. *Front Pharmacol* 2022; 13: 827896.
17. Chai Y, Zhu K, Li C, et al. Dexmedetomidine alleviates cisplatininduced acute kidney injury by attenuating endoplasmic reticulum stressinduced apoptosis via the alpha2AR/PI3K/AKT pathway. *Mol Med Rep* 2020; 21: 1597–1605.
18. Sugishita K, Su Z, Li F, et al. Gender influences [Ca(2+)](i) during metabolic inhibition in myocytes overexpressing the Na(+)-Ca(2+) exchanger. *Circulation* 2001; 104: 2101–2106.
19. Duong E, Xiao J, Qi XY, et al. MicroRNA-135a regulates sodium-calcium exchanger gene expression and cardiac electrical activity. *Heart Rhythm* 2017; 14: 739–748.
20. Yan M, Liu T, Zhong P, et al. Chronic catestatin treatment reduces atrial fibrillation susceptibility via improving calcium handling in post-infarction heart failure rats. *Peptides* 2023; 159: 170904.
21. Ni L, Zhou C, Duan Q, et al. beta-AR blockers suppresses ER stress in cardiac hypertrophy and heart failure. *PLoS One* 2011; 6: e27294.
22. Dalal S, Foster CR, Das BC, et al. Beta-adrenergic receptor stimulation induces endoplasmic reticulum stress in adult cardiac myocytes: role in apoptosis. *Mol Cell Biochem* 2012; 364: 59–70.
23. Meng D, Feng L, Chen XJ, et al. Trimetazidine improved Ca2+ handling in isoprenaline-mediated myocardial injury of rats. *Exp Physiol* 2006; 91: 591–601.
24. Chen S, Du J, Liang Y, et al. Sulfur dioxide restores calcium homeostasis disturbance in rat with isoproterenol-induced myocardial injury. *Histol Histopathol* 2012; 27: 1219–1226.
25. Bers DM. Cardiac excitation-contraction coupling. *Nature* 2002; 415: 198–205.
26. Bers DM. Altered cardiac myocyte Ca regulation in heart failure. *Physiology* 2006; 21: 380–387.
27. Curran J, Hinton MJ, Rios E, et al. Beta-adrenergic enhancement of sarcoplasmic reticulum calcium leak in cardiac myocytes is mediated by calcium/calmodulin-dependent protein kinase. *Circ Res* 2007; 100: 391–398.
28. Shen JX. Isoprenaline enhances local Ca2+ release in cardiac myocytes. *Acta Pharmacol Sin* 2006; 27: 927–932.
29. Baier MJ, Noack J, Seitz MT, et al. Phosphorylation of RyR2 Ser-2814 by CaMKII mediates beta1-adrenergic stress induced Ca(2+) -leak from the sarcoplasmic reticulum. *FEBS Open Bio* 2021; 11: 2756–2762.
30. Liu X, Wang S, Guo X, et al. Increased Reactive Oxygen Species-Mediated Ca(2+)/Calmodulin-Dependent Protein Kinase II Activation Contributes to Calcium Handling Abnormalities and Impaired Contraction in Barth Syndrome. *Circulation* 2021; 143: 1894–1911.
31. Benitah JP, Perrier R, Mercadier JJ, et al. RyR2 and Calcium Release in Heart Failure. *Front Physiol* 2021; 12: 734210.
32. Mustroph J, Wagemann O, Lucht CM, et al. Empagliflozin reduces Ca/calmodulin-dependent kinase II activity in isolated ventricular cardiomyocytes. *ESC Heart Fail* 2018; 5: 642–648.
33. Dong S, Teng Z, Lu FH, et al. Post-conditioning protects cardiomyocytes from apoptosis via PKC(epsilon)-interacting with calcium-sensing receptors to inhibit endo(sarco)plasmic reticulum-mitochondria crosstalk. *Mol Cell Biochem* 2010; 341: 195–206.
34. George I, Sabbah HN, Xu K, et al. beta-adrenergic receptor blockade reduces endoplasmic reticulum stress and

normalizes calcium handling in a coronary embolization model of heart failure in canines. *Cardiovasc Res* 2011; 91: 447–455.
35. Castillero E, Akashi H, Pendrak K, et al. Attenuation of the unfolded protein response and endoplasmic reticulum stress after mechanical unloading in dilated cardiomyopathy. *Am J Physiol Heart Circ Physiol* 2015; 309: H459–470.
36. Wang M, Sun GB, Zhang JY, et al. Elatoside C protects the heart from ischaemia/reperfusion injury through the modulation of oxidative stress and intracellular Ca(2)(+) homeostasis. *Int J Cardiol* 2015; 185: 167–176.
37. Zhuo XZ, Wu Y, Ni YJ, et al. Isoproterenol instigates cardiomyocyte apoptosis and heart failure via AMPK inactivation-mediated endoplasmic reticulum stress. *Apoptosis* 2013; 18: 800–810.
38. Gong W, Duan Q, Cai Z, et al. Chronic inhibition of cGMP-specific phosphodiesterase 5 suppresses endoplasmic reticulum stress in heart failure. *Br J Pharmacol* 2013; 170: 1396–1409.
39. Krenek P, Kmecova J, Kucerova D, et al. Isoproterenol-induced heart failure in the rat is associated with nitric oxide-dependent functional alterations of cardiac function. *Eur J Heart Fail* 2009; 11: 140–146.
40. Qin M, Liu T, Hu H, et al. Effect of isoprenaline chronic stimulation on APD restitution and ventricular arrhythmogenesis. *J Cardiol* 2013; 61: 162–168.
41. Lee Y and Gustafsson AB. Role of apoptosis in cardiovascular disease. *Apoptosis* 2009; 14: 536–548.
42. Fan CL, Yao ZH, Ye MN, et al. Fuziline alleviates isoproterenol-induced myocardial injury by inhibiting ROS-triggered endoplasmic reticulum stress via PERK/eIF2alpha/ATF4/Chop pathway. *J Cell Mol Med* 2020; 24: 1332–1344.
43. Davlouros PA, Gkizas V, Vogiatzi C, et al. Calcium Homeostasis and Kinetics in Heart Failure. *Med Chem* 2016; 12: 151–161.
44. Grassi G, Seravalle G, Bertinieri G, et al. Sympathetic and reflex abnormalities in heart failure secondary to ischaemic or idiopathic dilated cardiomyopathy. *Clin Sci (Lond)* 2001; 101: 141–146.
45. Chen SL, Hu ZY, Zuo GF, et al. I(f) current channel inhibitor (ivabradine) deserves cardioprotective effect via down-regulating the expression of matrix metalloproteinase (MMP)-2 and attenuating apoptosis in diabetic mice. *BMC Cardiovasc Disord* 2014; 14: 150.
46. Han S, Hagan DL, Taylor JR, et al. Dapagliflozin, a selective SGLT2 inhibitor, improves glucose homeostasis in normal and diabetic rats. *Diabetes* 2008; 57(6): 1723–1729.
47. Elkazzaz SK, Khodeer DM, El Fayoumi HM, et al. Role of sodium glucose cotransporter type 2 inhibitors dapagliflozin on diabetic nephropathy in rats; Inflammation, angiogenesis and apoptosis. *Life Sci* 2021; 280: 119018.
48. Arab HH, Safar MM and Shahin NN. Targeting ROS-Dependent AKT/GSK-3β/NF-κB and DJ-1/Nrf2 Pathways by Dapagliflozin Attenuates Neuronal Injury and Motor Dysfunction in Rotenone-Induced Parkinson's Disease Rat Model. *ACS Chem Neurosci* 2021; 12(4): 689–703.